Received: 27 April 2023 | Revised: 26 July 2023 | Accepted: 27 July 2023

DOI: 10.1002/mgg3.2268

Molecular Genetics & Genomic Medicine Open Access WILEY

ORIGINAL ARTICLE

Clinical report and genetic analysis of a Chinese neonate with craniofacial microsomia caused by a splicing variant of the splicing factor 3b subunit 2 gene

Yongli Zhang[1] | Shaohua Bi[1] | Liying Dai[1] | Yuwei Zhao[1] | Yu Liu[1] | Zifeng Shi[2]

[1]Department of Neonatology, Children's Hospital of Fudan University at Anhui (Anhui Provincial Children's Hospital), Hefei, Anhui Province, China

[2]Center of Imaging Diagnosis, Children's Hospital of Fudan University at Anhui (Anhui Provincial Children's Hospital), Hefei, Anhui Province, China

Correspondence
Yongli Zhang, Department of Neonatology, Children's Hospital of Fudan University at Anhui (Anhui Provincial Children's Hospital), Hefei, Anhui Province, China.
Email: zhangyongli_23@163.com

Abstract

Background: Craniofacial microsomia (CFM) is a common congenital malformation with unknown pathogenesis. Although few cases have been reported, it is suggested that variants of the *SF3B2* gene may lead to CFM. We herein report the case of a neonate with CFM exhibiting rare features of airway obstruction.

Methods: Trio whole-exome sequencing and Sanger validation were performed on the proband and her parents. Candidate gene mutations were analyzed using the Genome Aggregation Database (gnomAD) for normal frequency distributions. The Human Splicing Finder (HSF) and Rare Disease Data Center (RDDC) RNA splicer algorithms predicted the variant's harmfulness, verified by a Minigene assay.

Results: The proband had a heterozygous *SF3B2* variant, NM_006842.3:c.777+1G>A. The patient's father also carried this variant and exhibited facial abnormalities. The variant was not in gnomAD, and HSF and RDDC RNA splicers indicated donor site disruption. The minigene assay suggested that two mRNA products were produced, leading to a premature termination codon.

Conclusion: For this family, the pathogenesis of CFM may have been caused by an *SF3B2* splicing variant. Affected family members exhibited varying degrees of malformation, indicating that CFM has phenotypic heterogeneity. This finding expands the phenotype and variant spectrum of *SF3B2*, enriches neonatal CFM research, and provides a possible guide to genetic counseling.

KEYWORDS

craniofacial microsomia, *SF3B2* gene variants, whole-exome sequencing

1 | INTRODUCTION

Craniofacial microsomia (CFM; OMIM # 164210) is the second most common congenital craniofacial malformation after cleft lip/palate. The global incidence rate is approximately 1/5000–1/3000 (Birgfeld & Heike, 2019). CFM is a structural-developmental disorder usually occurring in the first and second branchial arches around the fourth to sixth week of pregnancy. Its prominent features include hypoplasia of the mandible and maxilla, ear, orbit,

and facial nerves (Timberlake, 2021). Ear malformations are characteristic of CFM, ranging from microtia or incomplete auricles to preauricular skin tags. In addition, severe CFM phenotypes can include epibulbar dermoids, vertebral malformations, and lung, brain, and urogenital abnormalities, forming a syndrome (Kuu-Karkku et al., 2023). The pathogenesis of CFM is complex and is related to neural crest (NC) cells migration and patterning, fibroblast growth factor receptor signal transduction, ribosomal assembly, and abnormal chromatin modification (Gebuijs et al., 2022; Park et al., 2022; Pulman et al., 2019; Shull et al., 2020).

Variants in genes associated with spliceosomal defects (such as *EFTUD2*, *TXNL4A*, and *SF3B4*) can lead to craniofacial malformations (Cox et al., 2014). The spliceosome is a large ribonucleoprotein complex that participates in the cleavage of introns in pre-mRNA transcripts and is a key link between gene transcription and protein translation processes (Lehalle et al., 2015). Timberlake et al. (2021) recently discovered that there is a correlation between the loss-of-function (LOF) variant of the splicing factor 3b subunit 2 (*SF3B2*, OMIM # 605591) gene and CFM. They found that four out of 77 families with microtia carry LOF variants of the *SF3B2* gene. Therefore, *SF3B2* gene variants may be associated with a higher incidence of CFM.

Here, we report the case of a Chinese family with CFM and a neonatal proband characterized by craniofacial malformation, feeding difficulties, and respiratory failure caused by airway obstruction. The case was suggested to be caused by a *SF3B2* splicing mutation based on whole-exome sequencing. This study expands on the *SF3B2* variant clinical implications and suggests that *SF3B2* variants should be considered in neonatal and perinatal CFM.

2 | METHODS

2.1 | Editorial policies and ethical considerations

In October 2022, we recruited a Chinese family with CFM comprising three generations and five members. All family members participating in this study provided written informed consent and agreed to disclose imaging, clinical, and genetic data. Parents or guardians provided informed consent for participants under the age of 18 years. This study was approved by the Medical Ethics Committee of Anhui Provincial Children's Hospital (EYLL-2017-023).

2.2 | Whole-exome sequencing

Trio whole-exome sequencing was performed for the proband and her parents. First, peripheral venous blood was collected, and after anticoagulation treatment with ethylenediaminetetraacetic acid, genomic DNA was extracted according to the genome extraction kit instructions (Qiagen, Hilden, Germany). A sequencing library was prepared, and the target sequence was captured using the xGen Exome Research Panel v2.0 (IDT). The target sequence was paired-end sequenced (150 bp, WeHealth BioMedical) using an Illumina NovaSeq 6000 high-throughput sequencing platform (Illumina). The read data were mapped to the University of California Santa Cruz Genome Browser (hg19), and the Genome Analysis Toolkit v4.1.9 software identified mutation sites (McKenna et al., 2010). The minor allele frequency was defined using the Genome Aggregation Database (gnomAD; http://gnomad-old.broadinstitute.org/). The variant's pathogenicity was determined using the American College of Medical Genetics and Genomics (ACMG) guidelines (Richards et al., 2015).

2.3 | Sanger sequencing

Sanger sequencing was performed for the proband and her parents. The mutation primers were designed according to the Ensembl database (http://ensemblgenomes.org/). The primer sequence was F: 5′-TACACACTGAACACACTGTACAAC-3′, R: 5′-GGACCCCAACACGACTCTGCCT-3′. Amplification was performed using the following conditions: one cycle at 95°C for 2 min, followed by 39 cycles at 95°C for 30 s, 60°C for 30 s, 72°C for 40 s, and a final extension at 72°C for 5 min. The amplified products were sequenced using the ABI 3730XL automatic sequencer (Thermo Fisher Scientific).

2.4 | In-silico analysis

Two visualization software packages were used for online analysis of splice variant harmfulness: the Rare Disease Data Center (RDDC) RNA Splicer (https://rddc.tsinghua-gd.org/; Jaganathan et al., 2019) and the Human Splicing Finder (HSF) v3.0 (https://www.genomnis.com/access-hsf) (Desmet et al., 2009). These software packages were used to evaluate the potential strength of the new/cryptic splicing sites in the *SF3B2* gene variant.

2.5 | Minigene

The minigene plasmid was designed with an insertion between the exon6 and exon8 sequences of the *SF3B2* gene and the gDNA primer sequences SF3B2-F: 5′-AAGCTGGTACCGAGCTGGATCCGCCAGCTGTTTACTGGAGGAGAGAACGAC-3′ and SF3B2-R: 5′-TTAAA

CGGGCCCTCTAGACTCGAGCCTGCTGAGAATTC ATCTCTTCCTGG-3′ were amplified. The amplified products were cloned into the pMini-CopGFP vector (Hitrobio Biotechnology) using the ClonExpress II One-Step Cloning Kit (Vazyme) and restriction endonuclease 5′-BamHI/3′-XhoI. Variant plasmids were obtained through site-specific mutagenesis using SF3B2-MUT-F/R primers (SF3B2-MT-F: 5′-ACAGAGaTGAGACTGATT TATTCCTAGGGA-3′; SF3B2-MT-R: 5′-CAGTCATCTCT GTTCATCTCCAGG-3′) based on wild-type plasmids. The wild-type and variant plasmids of the minigene were verified by Sanger sequencing.

Human 293T cells were grown to 80% confluence in a 6-well plate and were transiently transfected with Lipofectamine 2000 (Invitrogen). Total RNA was extracted from the cells using the TRIzol reagent (Cowin Biotech), cDNA was synthesized from the extracted RNA using HiScript II 1st Strand cDNA Synthesis Kit (+gDNA wiper; Cat#R212-01, Vazyme Biotech Co., Ltd.). MiniRT-F (5′-GCTAACTAGAACCCACTGCTTA-3′) and SF3B2-RT-R primers (5′-CCTGAGAATTCATCTTCCT-3′) were designed for PCR amplification with amplification parameters of 98°C for 10 s, 60°C for 30 s, and 68°C for 30 s, for a total of 30 cycles. The amplified product was detected by 3% agar gel electrophoresis and sequenced in ABI 3730 XL (Applied Biosystems). ExPASy-translate (https://web.expasy.org/translate/) translated nucleotide sequences into protein sequences and analyzed the impact of the variant on the translation process.

3 | RESULTS

3.1 | Case presentation

The proband patient was a 4-day-old female newborn admitted to the neonatal intensive care unit because of intermittent cyanosis of the skin after birth. The patient was her mother's first child; the mother underwent a cesarean section at 38^{+2} weeks of pregnancy owing to intrauterine growth restriction and excessive amniotic fluid. The birth weight was 2620 g, and the Apgar score was 7 at 1 min and 10 at 5 min. At birth, a large amount of amniotic fluid, battledore placenta, and placenta previa were observed. The patient had congenital craniofacial anomalies that manifested as a transverse facial cleft, dysplasia of the auricle and external auditory canal, and neonatal bronchopneumonia.

Physical examination revealed that the patient was conscious, and the frontal fontanel was flat and soft. Ear position was low bilaterally, and accessory auricles were present. Atypical facial features included a large mouth, with the right corner of the mouth opening horizontally to the cheek and a hard granular mass visible on the outer right corner of the mouth. The patient also had a cleft palate that extended from the uvula to the junction of the soft and hard palates, with a width of approximately 1.5 cm. The mandible was short and skewed, with the base of the tongue falling back (Figure 1a–d). The neck was soft, the respiratory rate was 66 breaths/min, the three depressions

FIGURE 1 Facial features of the patient and affected family members. (a) The patient's facial manifestation includes a large mouth, with the right corner horizontal to the cheek (yellow arrow), and the lower jaw is short and tilted to the left. (b) A cleft palate can be seen (yellow arrow). (c) The ear position is low on the right side, with accessory ears (yellow arrow). A lump can be seen on the outer side of the right corner of the mouth, which is hard (red arrow). (d) On the left side, the ear position is low, with the presence of accessory ears (yellow arrow). (e) The patient's father's left auricle is malformed without access to the normal ear canal (yellow arrow). (f) The father has an accessory ear on the right side, and the auricle and auditory canal are normal. Surgical scars can be seen on the right cheek (red arrow). (g) The patient's grandmother has an accessory ear visible on the left side (yellow arrow). (h) The grandmother has an accessory ear on the right side (yellow arrow) and congenital aural atresia.

sign was positive, and the respiratory sounds in both lungs were rough. Grade II/6 systolic murmurs were heard in the precordium. No other obvious physical abnormalities were observed, including hepatosplenomegaly, abnormal limb mobility, or abnormal muscle tone. Laboratory examination and blood gas analysis indicated that the patient had type 2 respiratory failure caused by airway obstruction (with a partial pressure of carbon dioxide [PCO_2] at 51.7 mmHg and a partial pressure of oxygen at 74.9 mmHg under oxygen inhalation). Routine blood examinations revealed no additional obvious abnormalities. Computed tomography (CT) revealed glossoptosis, a narrow oropharynx, and a short mandible (Figure 2). A chest and spine CT showed no apparent abnormalities.

The patient's parents were non-consanguineous. The patient's father had an asymmetric face with a deformed left auricle and an inaccessible auditory meatus. An accessory auricle was observed on the right side. The patient's grandmother also had an accessory auricle on both sides with right ear canal atresia (Figure 1e–h). Other family members had no abnormal facial features or ears.

3.2 | Genetic testing

For the proband, the average sequencing depth of the target area was 132.2 X, with an average sequencing depth of ≥10 X and a coverage of 99.13%. After the screening, the *SF3B2* gene of the proband was determined to be a heterozygous variant, NM_006842.3: c.777+1G>A, which was inherited from her father. Her mother carried the wild-type gene. This variant was not included in gnomAD and was a novel variant yet to be reported. Sanger sequencing confirmed that the proband and her father carried the variant, and the mother carried the wild-type gene (Figure 3). The ACMG rated the mutation as having uncertain significance.

FIGURE 2 Computed tomography (CT) scan and three-dimensional (3D) imaging of the patient's jaw. (a) Sagittal CT showing glossoptosis, a narrow oropharynx airway (red arrow), and a short mandibular body (yellow arrow). (b) 3D imaging shows that the right mandible is short and small. (c) The left mandible is shorter and smaller than the right.

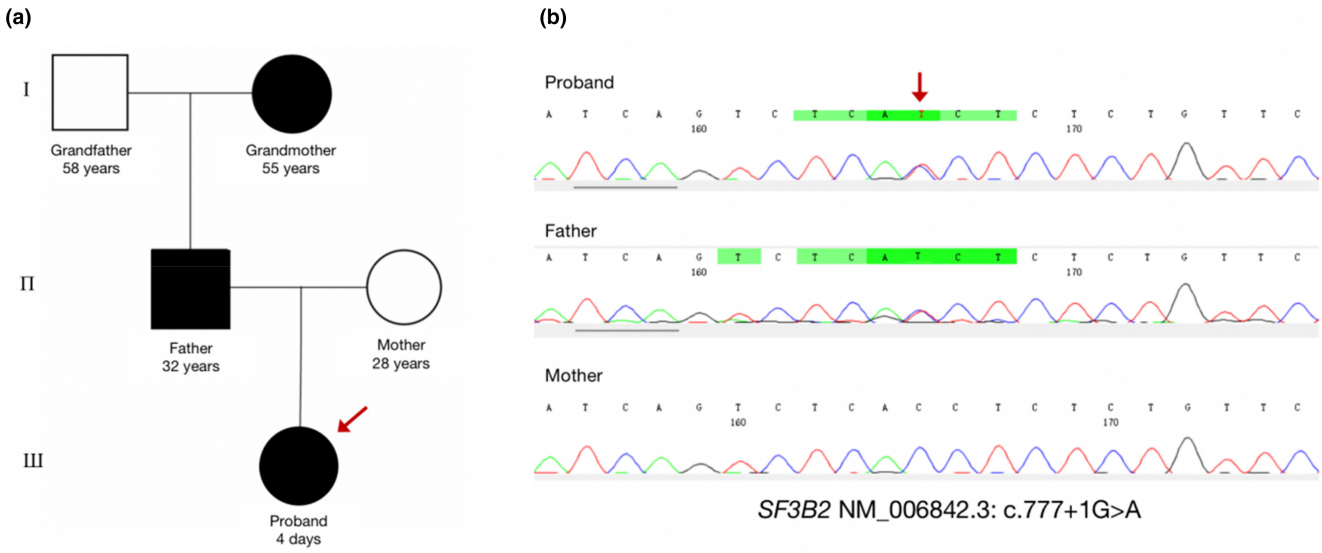

FIGURE 3 The patient's pedigree and Sanger results. (a) The patient's pedigree. Affected family members are marked in red, and the proband is indicated by a red arrow. (b) The genetic testing results indicate an NM_006842.3: c.777+1G>A *SF3B2* gene variant, which was inherited from the father. The mother carried the wild-type gene.

3.3 | Predicting splicing disruptions

The HSF prediction included two algorithms (HSF Matrix and MaxEnt), and the results showed that c.777+1G>A can disrupt the wild-type donor site and generate new variable splicing sites (Table 1). The predicted results of the RDDC RNA splicer indicated that c.777+1G>A can generate three splicing modes: (1) insertion of 387 bp, promoting an alternative splicing donor; (2) exon 7 missing 110 bp, resulting in exon skipping; and (3) insertion of the entire segment of exon 7 at 678 bp, resulting in a premature termination codon (Supplementary Material).

TABLE 1 Human Splicing Finder v3.0 predicted the c.777+1G>A variant of the *SF3B2* gene.

HSF algorithm	HSF matrix	MaxEnt
Position	Chr11:66057373	Chr11:66057373
Sequence Reference	GAGGTGAGA	GAGGTGAGA
Sequence Mutation	GAGATGAGA	GAGATGAGA
Score Reference	93.37	7.66
Score Mutation	66.23	−0.53
Delta	−29.07%	−106.92%
Results	Site Donor Broken	Site Donor Broken

Abbreviation: HSF, Human Splicing Finder.

3.4 | Minigene experiment

The variant plasmid transcribed two mRNA products, the first being exon 7 with a complete deletion of the 110 bp sequence, resulting in exon skipping and a frameshift mutation, leading to a premature termination codon. The variant expression mode was NM_006842.3: c.668_777del (p.Val223AspfsTer3). The second product was exon 7 with a complete deletion of a 110-bp sequence while partially retaining a 67-bp sequence of intron 6. This frameshift variant leads to a premature termination codon, and the expression of the variant is NM_006842.3: c.668_777del, c.667+1_667+67 ins (p.Val223GlyfsTer15). Compared with the wild-type plasmid transcriptional mRNA sequence, it contained the complete exons 6–8 (Figure 4).

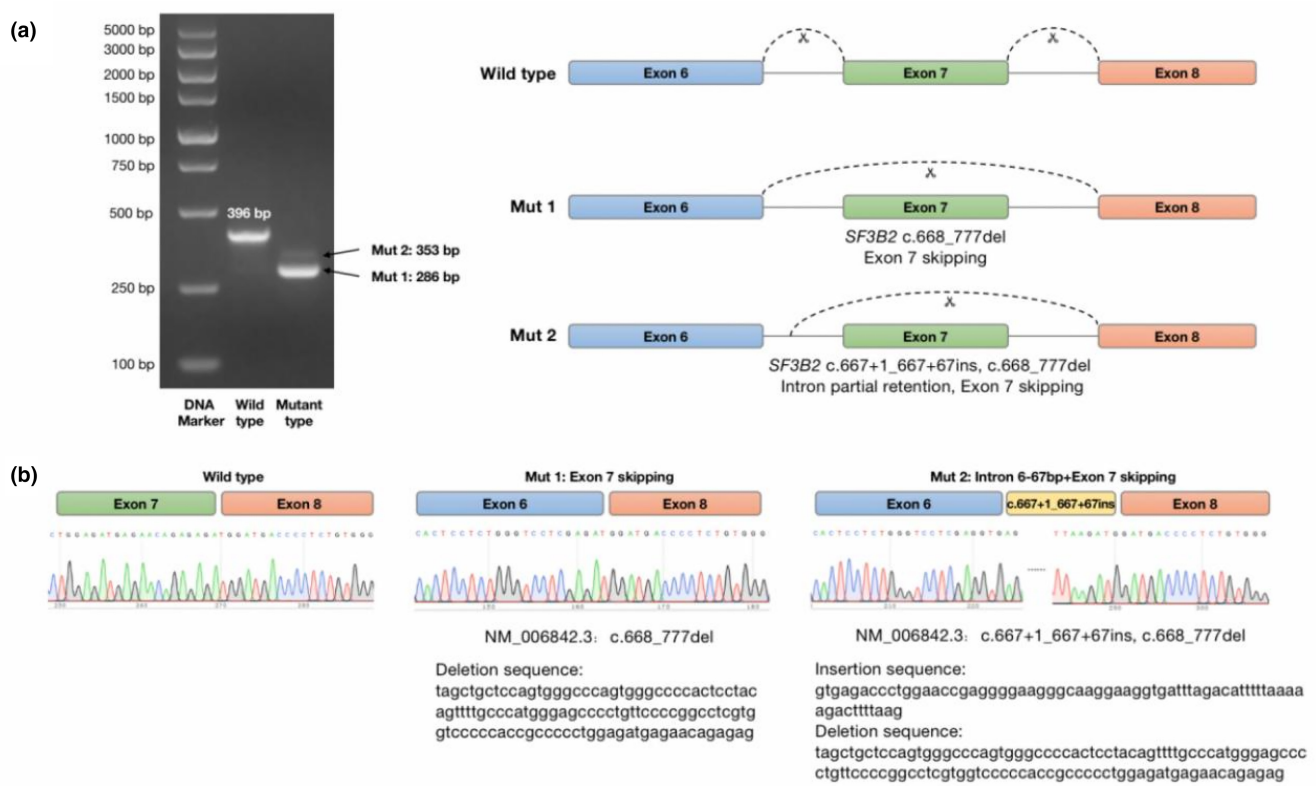

FIGURE 4 In vitro Minigene experiment. (A) The Minigene assay was conducted to construct the *SF3B2* gene with c.777+1G>A. The electrophoresis pattern shows two bands (Mut 1 and Mut 2) in the variant, indicating two mRNA products. The first product (Mut 1) is a complete deletion of the 110 bp sequence in exon 7, leading to exon skipping. The expression pattern of the variant is NM_006842.3: c.668_777del (p.Val223AspfsTer3). The second product (Mut 2) is exon 7 with a complete deletion of the 110 bp sequence while partially retaining the 67 bp sequence of intron 6. The variant expression is NM_006842.3: c.668_777del, c.667+1_667+67ins (p.Val223GlyfsTer15). Wild-type plasmids transcribe mRNA sequences containing complete exons 6–8. (B) Sanger sequencing results and the Mut 1 deletion and Mut 2 insertion/deletion sequences.

4 | DISCUSSION

The patient had a craniofacial disorder since birth, characterized by a transverse rupture of the right corner of the mouth to the cheek and visible granular masses. She also had a cleft palate, mandibular dysplasia, a low ear position, and accessory ears. These findings were similar to those of previously reported patients with CFM (Timberlake, 2021). We have summarized the clinical findings from previous reports, which indicate that the main manifestations among different individuals include external ear malformation and mandibular hypoplasia. Therefore, patients often exhibit micrognathia and hearing impairment (Table 2). In our patient, there was mandibular hypoplasia and posterior displacement of the tongue base, which may have contributed to airway obstruction and subsequent carbon dioxide retention, leading to elevated PCO_2 levels. Similar respiratory failure characteristics resulting from severe mandibular aplasia have not been reported in other patients with CFM.

Genetic testing showed that the patient and her father had a c.777+1G>A variant in the *SF3B2* gene, which is a novel variant. Although the patient's grandmother did not undergo genetic testing, it was speculated that she also carried the variant due to the presence of ear malformations. We used predictive software programs to analyze the variant, which revealed that the wild-type donor site may be disrupted, leading to a premature termination codon. The in vitro Minigene experiment confirmed this prediction; after cloning and sequencing, the splicing variant produces two mRNA products and may result in truncated proteins. Our study further demonstrated that LOF mutations in the *SF3B2* gene led to haploinsufficiency and CFM (Timberlake et al., 2021) and provided clinical data for neonatal patients and families with CFM.

The *SF3B2* gene is located on 11q13.1 and spans 22 exons. It encodes subunit 2 of the splicing factor 3b (SF3B) protein

TABLE 2 Reported clinical and genetic characteristics of patients with *SF3B2*-related CFM.

	1	2	3	4–1
Sex	F	M	M	F
Age at diagnosis	17 years	9 years	10 years	12 years
Jaw abnormalities	Mild hypoplasia of the L jaw	Moderate underdevelopment of the R upper jaw, lower jaw, and cheekbones	Moderate hypoplasia of the R upper and lower jaw	Moderate hypoplasia of the L upper and lower jaw
Facial transversal cleft	—	—	R	L
Ear deformity	L tragus duplication	R tragus duplication	Bi tragus duplication	L external auditory canal atresia
Hearing	Normal	R hearing loss	Normal	L hearing loss
Ophthalmic phenotype	Myopia	—	—	Ptosis
Skeletal phenotype	Bi cervical ribs	L cervical rib	Bi cervical ribs	Spinal abnormalities
Cardiac phenotype	Loss of L pulmonary artery, abnormal L subclavian artery, R aortic arch	/	—	Ventricular septal defect
Congenital disability	—	—	—	Cleft palate, torticollis, abnormal anal position, sparse hair
Nucleic acid alteration (NM_006842.3)	c.2329dupG	c.2480dupC	c.1780->-	c.1608dupG
Amino acid alteration	p.Asp776GlufsX4	p.Ala827ArgfsX5	/	p.Arg537AlafsX24
Inheritance	De novo	Paternal	De novo	/

Abbreviations: —, No phenotype; /, Not Available; Bi, bilateral; CFM, craniofacial microsomia; F, female; L, left; M, male; R, right.

complex, which is comprised of 895 amino acids. SF3B2 performs biological splicing by forming the SF3B heptamer complex with six other subunits (SF3B1, SF3B3, SF3B4, SF3B5, SF3B6, and SF3B7) (Das et al., 1999; Will et al., 2001, 2002). The SF3B complex is an important component of the U2 small nuclear riboprotein complex (U2 snRNP), which binds to pre-mRNAs upstream of intron-branching sites and anchors U2 snRNPs onto pre-mRNAs (Timberlake et al., 2021). The SF3B2 protein may come into contact with the C-terminal HEAT domain of SF3B1 through the HEAT interaction domain, and SF3B4 is connected to the middle part of the SF3B complex to achieve pre-mRNA anchoring (Timberlake et al., 2021; Will et al., 2002). The novel variant identified in this study may affect protein expression and interfere with its biological function.

To date, only eight patients with *SF3B2*-related CFM have been reported (Table 2). Notably, most patients had unilateral abnormal features, including two with unilateral transverse facial clefts and three with unilateral external auditory canal malformations. The family with CFM in this study also had similar characteristics, with the patient's right corner of the mouth opening horizontally to the cheek and, along with her father and grandmother, unilateral external auditory canal malformations. This condition differs from Nager syndrome (NS, OMIM:154400), which is associated with the *SF3B4* gene. Although SF3B4 interacts with SF3B2 to form a part of the SF3B complex, NS can cause symmetrical deformities in the face and mandible (Cretu et al., 2016). The mechanism of *SF3B2* gene defects leading to unilateral craniofacial malformations in humans is still unclear. Timberlake et al. (2021) hypothesized that it may be caused by genetic modifiers of somatic cell presentation or "second hits" of somatic cells; that is, *SF3B2* has an allelic germline variant accompanied by somatically acquired inactivation of the second allele. Further research on *SF3B2* somatic cell variants and the potential mechanisms of genetic modifiers in the patient population with CFM is required.

4–2	5–1	5–2	6	Our study
M	F	M	F	F
17 years	30 years	28 years	1.5 years	4 days
Mild hypoplasia of the L upper and lower jaw	L maxillary, mandibular, and zygomatic dysplasia	—	—	Short and skewed mandible
—	Bi	—	—	R
Bi microtia	Bi microtia, absent R tragus, accompanied by external auditory canal atresia	—	—	Bi-low ear position and tragus duplication
Normal	Bi hearing loss	Congenital perforation of L tympanic membrane	Normal	Failure to pass newborn hearing test
Amblyopia and strabismus	R epibulbar dermoid	—	Right exotropia, hyperopia, ptosis	—
Extra flexion creases on both sides of the thumb, knee valgus	—	—	L bifid thumb	—
—	/	/	/	Patent foramen ovale
Premature adrenarche, mild skin syndactyly of digits	—	—	Mild skin syndactyly of toes	Intrauterine growth restriction, cleft palate, oropharyngeal airway stenosis
c.1608dupG	c.1912C>T	c.1912C>T	c.307C>T	c.777+1G>A
p.Arg537AlafsX24	p.Arg638X	p.Arg638X	p. Gln103X	/
/	De novo	De novo	/	Paternal

The lack of NC cells in the craniofacial region is believed to be the pathological basis of craniofacial disorders, particularly mandibular and external auditory canal deformities (Birgfeld & Heike, 2019). Disease-causing variants in genes encoding spliceosome proteins are called spliceosomopathies. These genes include *SF3B4*, *EFTUD2*, *TXNL4A*, and *SNRPB*, which are crucial for NC cells and craniofacial development (Bernier et al., 2012). In a *Xenopus* model with *SF3B2* gene knockdown, NC cell formation and development were disrupted, indicating that early depletion of NC cells may contribute to CFM occurrence (Timberlake, 2021). Owing to common etiological mechanisms, the phenotypes of different diseases also overlap; for example, children with NS have similar facial, ear, and mandibular deformities (Cretu et al., 2016). Accordingly, pediatricians, especially neonatologists, are required to differentiate and diagnose *SF3B2*-related CFM.

5 | CONCLUSIONS

In conclusion, we report a rare case of CFM in a neonatal patient who not only presented with unilateral facial and ear deformities and a small mandible but also exhibited previously unreported symptoms of type 2 respiratory failure caused by airway obstruction. Genetic testing results indicated a splicing variant of the *SF3B2* gene, confirmed with bioinformatics software and in vitro Minigene experiments, leading to a premature termination codon. Clinically, there were phenotypic differences among family members carrying variants, indicating that CFM has phenotypic heterogeneity. Expanding the CFM cohort can help reveal the association between phenotype and genotype and explore the potential mechanisms underlying the high incidence of unilateral craniofacial malformations in patients with CFM.

AUTHOR CONTRIBUTIONS

Yongli Zhang drafted the work. Yongli Zhang and Shaohua Bi acquired and analyzed the data and drafted the work. Yongli Zhang, Shaohua Bi, Yu Liu, and Zifeng Shi provided technical and methodological support. Yongli Zhang, Yu Liu, and Zifeng Shi contributed to the collation of patient's clinical data. Liying Dai and Yongli Zhang contributed to the conception of the work and revised it critically for important intellectual content. All authors approved the publication of the content.

ACKNOWLEDGMENTS

We thank the patient and her family for participating in this study.

FUNDING INFORMATION

This research received no specific grant from funding agencies in the public, commercial, or not-for-profit sectors.

CONFLICT OF INTEREST STATEMENT

The authors declare that there are no conflicts of interest.

DATA AVAILABILITY STATEMENT

The authors confirm that the data supporting the findings of this study are available within the article and its supplementary materials.

ETHICS APPROVAL STATEMENT

This study was approved by the Medical Ethics Committee of Anhui Provincial Children's Hospital (EYLL-2017-023).

PATIENT CONSENT STATEMENT

All family members participating in this study provided written informed consent and agreed to disclose imaging, clinical, and genetic data. Parents or guardians provided informed consent for all participants under the age of 18 years.

ORCID

Yongli Zhang https://orcid.org/0009-0003-7441-4687

REFERENCES

Bernier, F. P., Caluseriu, O., Ng, S., Schwartzentruber, J., Buckingham, K. J., Innes, A. M., Jabs, E. W., Innis, J. W., Schuette, J. L., Gorski, J. L., Byers, P. H., Andelfinger, G., Siu, V., Lauzon, J., Fernandez, B. A., McMillin, M., Scott, R. H., Racher, H., Consortium, F. O. R. G. E. C., … Parboosingh, J. S. (2012). Haploinsufficiency of SF3B4, a component of the pre-mRNA spliceosomal complex, causes Nager syndrome. *American Journal of Human Genetics*, *90*(5), 925–933. doi:10.1016/j.ajhg.2012.04.004

Birgfeld, C., & Heike, C. (2019). Craniofacial microsomia. *Clinics in Plastic Surgery*, *46*(2), 207–221. doi:10.1016/j.cps.2018.12.001

Cox, T. C., Camci, E. D., Vora, S., Luquetti, D. V., & Turner, E. E. (2014). The genetics of auricular development and malformation: New findings in model systems driving future directions for microtia research. *European Journal of Medical Genetics*, *57*(8), 394–401. doi:10.1016/j.ejmg.2014.05.003

Cretu, C., Schmitzová, J., Ponce-Salvatierra, A., Dybkov, O., De Laurentiis, E. I., Sharma, K., Will, C. L., Urlaub, H., Lührmann, R., & Pena, V. (2016). Molecular architecture of SF3b and structural consequences of its cancer-related mutations. *Molecular Cell*, *64*(2), 307–319. doi:10.1016/j.molcel.2016.08.036

Das, B. K., Xia, L., Palandjian, L., Gozani, O., Chyung, Y., & Reed, R. (1999). Characterization of a protein complex containing spliceosomal proteins SAPs 49, 130, 145, and 155. *Molecular and Cellular Biology*, *19*(10), 6796–6802. https://doi.org/10.1128/MCB.19.10.6796

Desmet, F. O., Hamroun, D., Lalande, M., Collod-Béroud, G., Claustres, M., & Béroud, C. (2009). Human Splicing Finder: An online bioinformatics tool to predict splicing signals. *Nucleic Acids Research*, *37*(9), e67. https://doi.org/10.1093/nar/gkp215

Gebuijs, L., Wagener, F. A., Zethof, J., Carels, C. E., Von den Hoff, J. W., & Metz, J. R. (2022). Targeting fibroblast growth factor receptors causes severe craniofacial malformations in zebrafish larvae. *PeerJ*, *10*, e14338. https://doi.org/10.7717/peerj.14338

Jaganathan, K., Kyriazopoulou Panagiotopoulou, S., McRae, J. F., Darbandi, S. F., Knowles, D., Li, Y. I., Kosmicki, J. A., Arbelaez, J., Cui, W., Schwartz, G. B., Chow, E. D., Kanterakis, E., Gao, H., Kia, A., Batzoglou, S., Sanders, S. J., & Farh, K. K. (2019). Predicting splicing from primary sequence with deep learning. *Cell*, *176*(3), 535–548.e24. https://doi.org/10.1016/j.cell.2018.12.015

Kuu-Karkku, L., Suominen, A., & Svedström-Oristo, A. L. (2023). Craniofacial microsomia—More than a structural malformation. *Orthodontics and Craniofacial Research*, *26*(1), 117–122. https://doi.org/10.1111/ocr.12592

Lehalle, D., Wieczorek, D., Zechi-Ceide, R. M., Passos-Bueno, M. R., Lyonnet, S., Amiel, J., & Gordon, C. T. (2015). A review of craniofacial disorders caused by spliceosomal defects. *Clinical Genetics*, *88*(5), 405–415. https://doi.org/10.1111/cge.12596

McKenna, A., Hanna, M., Banks, E., Sivachenko, A., Cibulskis, K., Kernytsky, A., Garimella, K., Altshuler, D., Gabriel, S., Daly, M., & DePristo, M. A. (2010). The Genome Analysis Toolkit: A MapReduce framework for analyzing next-generation DNA sequencing data. *Genome Research*, *20*(9), 1297–1303. https://doi.org/10.1101/gr.107524.110

Park, B. Y., Tachi-Duprat, M., Ihewulezi, C., Devotta, A., & Saint-Jeannet, J. P. (2022). The core splicing factors EFTUD2, SNRPB and TXNL4A are essential for neural crest and craniofacial development. *Journal of Developmental Biology*, *10*(3), 29. https://doi.org/10.3390/jdb10030029

Pulman, J., Ruzzenente, B., Bianchi, L., Rio, M., Boddaert, N., Munnich, A., Rötig, A., & Metodiev, M. D. (2019). Mutations in the MRPS28 gene encoding the small mitoribosomal subunit protein bS1m in a patient with intrauterine growth retardation, craniofacial dysmorphism and multisystemic involvement. *Human Molecular Genetics*, *28*(9), 1445–1462. https://doi.org/10.1093/hmg/ddy441

Richards, S., Aziz, N., Bale, S., Bick, D., Das, S., Gastier-Foster, J., Grody, W. W., Hegde, M., Lyon, E., Spector, E., Voelkerding, K., Rehm, H. L., & Laboratory Quality Assurance Committee, A. C. M. G. (2015). Standards and guidelines for the interpretation of sequence variants: A joint consensus recommendation of the American College of Medical Genetics and Genomics and the Association for Molecular Pathology. *Genetics in Medicine*, *17*(5), 405–424. https://doi.org/10.1038/gim.2015.30

Shull, L. C., Sen, R., Menzel, J., Goyama, S., Kurokawa, M., & Artinger, K. B. (2020). The conserved and divergent roles of Prdm3 and Prdm16 in zebrafish and mouse craniofacial development. *Developmental Biology*, *461*(2), 132–144. https://doi.org/10.1016/j.ydbio.2020.02.006

Timberlake, A. T., Griffin, C., Heike, C. L., Hing, A. V., Cunningham, M. L., Chitayat, D., Davis, M. R., Doust, S. J., Drake, A. F., Duenas-Roque, M. M., Goldblatt, J., Gustafson, J. A., Hurtado-Villa, P., Johns, A., Karp, N., Laing, N. G., Magee, L., University of Washington Center for Mendelian Genomics, Mullegama, S. V., … Luquetti, D. V. (2021). Haploinsufficiency of SF3B2 causes craniofacial microsomia. *Nature Communications*, *12*(1), 4680. https://doi.org/10.1038/s41467-021-24852-9

Will, C. L., Schneider, C., MacMillan, A. M., Katopodis, N. F., Neubauer, G., Wilm, M., Lührmann, R., & Query, C. C. (2001). A novel U2 and U11/U12 snRNP protein that associates with the pre-mRNA branch site. *The EMBO Journal*, *20*(16), 4536–4546. https://doi.org/10.1093/emboj/20.16.4536

Will, C. L., Urlaub, H., Achsel, T., Gentzel, M., Wilm, M., & Lührmann, R. (2002). Characterization of novel SF3b and 17S U2 snRNP proteins, including a human Prp5p homologue and an SF3b DEAD-box protein. *The EMBO Journal*, *21*(18), 4978–4988. https://doi.org/10.1093/emboj/cdf480

SUPPORTING INFORMATION

Additional supporting information can be found online in the Supporting Information section at the end of this article.

How to cite this article: Zhang, Y., Bi, S., Dai, L., Zhao, Y., Liu, Y., & Shi, Z. (2023). Clinical report and genetic analysis of a Chinese neonate with craniofacial microsomia caused by a splicing variant of the splicing factor 3b subunit 2 gene. *Molecular Genetics & Genomic Medicine*, *11*, e2268. https://doi.org/10.1002/mgg3.2268